

Investigation of the eigenfrequencies of two interacting gas bubbles using the direct-numerical-simulation technique

Masato Ida

*Satellite Venture Business Laboratory, Gunma University,
1-5-1 Tenjin-cho, Kiryu-shi, Gunma 376-8515, Japan*

(Dated: February 9, 2020)

The recent theory regarding the eigenfrequencies of two mutually interacting gas bubbles in an acoustic field is verified numerically. The theory given by Ida [e-Print physics/0111133; (submitted)] predicts the existence of three eigenfrequencies per bubble, which make the phase difference between a bubble's pulsation and an external sound be $\pi/2$, while readymade theories predict only two natural frequencies. The direct-numerical-simulation technique, in which the compressible Navier-Stokes equation is selected as the governing equation, is employed for numerical experiments. We investigate the eigenfrequencies by observing the direction of the secondary Bjerknes force acting between pulsating bubbles, which changes as the driving frequency varies. The numerical results show that the theoretical prediction is valid at least in a qualitative sense.

PACS numbers: 43.20.+g, 47.55.Bx, 47.55.Dz

I. INTRODUCTION

The secondary Bjerknes force is an interaction force acting between pulsating gas bubbles in an acoustic field [1, 2, 3, 4, 5]. While the classical theory originated by Bjerknes [1, 2, 3] predicts only attraction or repulsion, recent studies show that the force sometimes reverses its own direction as the distance between the bubbles changes [4, 5]. The first theoretical study on this subject was performed by Zabolotskaya [4]. Employing a linear coupled-oscillator model, she showed that the radiative interaction between the bubbles could cause this reversal. In the middle of the 1990s, Doinikov and Zavtrak arrived at the same conclusion by employing a linear theoretical model in which the multiple scattering between the bubbles is more rigorously taken into account [5].

In both the theoretical studies mentioned above, it is assumed that the reversal is due to the change in the natural (or resonance) frequencies of bubbles caused by the radiative interaction between the bubbles. However, their interpretations on how the natural frequencies change differ from each other. The theoretical formula for the natural frequencies, used by Zabolotskaya, shows that higher and lower natural frequencies (converging to the partial natural frequencies of smaller and larger bubbles, respectively, when the distance between the bubbles is infinite) reveal upward and downward shifts, respectively, as the bubbles come closer to one another. On contrast, Doinikov and Zavtrak assumed intuitively that both natural frequencies rise. Although this assumption can explain the reversal occurring not only when both bubbles are larger than the resonance size but also when one bubble is larger than and the other is smaller than than the resonance size [5], it is in opposition to the theoretical interpretation by Zabolotskaya.

Recently, Ida proposed an alternative theoretical interpretation of this phenomenon [6], also using a linear model. He claimed that this phenomenon cannot be explained by using only the natural frequencies, and that it

is important to define the *eigenfrequencies* which make the phase difference between a bubble's pulsation and an external sound be $\pi/2$. It was pointed out theoretically that the number of the natural frequencies and that of the eigenfrequencies are not in agreement in a multibubble case [7, 8], while they are, as is well known, consistent in a single-bubble case. This theory can explain the reversal in both cases mentioned above, and does not contradict the theory for the natural frequencies used by Zabolotskaya. (In a double-bubble case, Ida's theory predicts three eigenfrequencies per bubble, two of which correspond to the natural frequencies [7].)

The aim of this paper is to verify the theory for the eigenfrequencies by direct numerical simulation (DNS). In Ref. [9], Ida and Yamakoshi proposed a DNS technique for multibubble dynamics in an acoustic field, in which the compressible Navier-Stokes equations with a surface-tension term are selected as the governing equation and are solved by semi-Lagrangian [10] and finite difference methods [9, 11]. This technique allows us to compute the dynamics (pulsation and translational motion) of deformable bubbles in a viscous liquid. (It seems that the solver for sound propagation, proposed in Ref. [9], may violate the conservation of mass greatly in a certain case [12]; we therefore employ a previous one [13] in this paper.) Using this DNS technique, we perform numerical experiments involving two interacting gas bubbles in order to investigate the recent theories by observing the pulsation amplitudes of bubbles and the direction of their translational motion. In Sec. II, the theories for the eigenfrequencies and secondary Bjerknes force are briefly reviewed, and in Sec. III, their numerical results and a discussion are provided.

II. THEORIES

Shima [14] and Zabolotskaya [4] derived the same formula for the natural frequencies of two interacting bub-

bles (bubbles 1 and 2), represented as

$$(\omega_{10}^2 - \omega^2)(\omega_{20}^2 - \omega^2) - \frac{R_{10}R_{20}}{D^2}\omega^4 = 0, \quad (1)$$

where ω_{10} and ω_{20} are the partial natural frequencies of bubbles 1 and 2, respectively, R_{10} and R_{20} are their equilibrium radii, ω is the driving (angular) frequency, and D is the distance between the centers of the bubbles. In their model used for deriving this equation, the sphericity of bubbles and the incompressibility of the surrounding liquid are assumed and the damping factors are neglected. This equation predicts the existence of two natural frequencies per bubble. The higher and the lower natural frequencies reveal upward and downward shifts, respectively, as the distance between the bubbles decreases.

The eigenfrequencies, defined by Ida [7], of bubble 1 are given by the following equation:

$$H_1 F + M_2 G = 0, \quad (2)$$

with

$$\begin{aligned} F &= L_1 L_2 - \frac{R_{10}R_{20}}{D^2}\omega^4 - M_1 M_2, \\ G &= L_1 M_2 + L_2 M_1, \quad H_1 = L_2 + \frac{R_{20}}{D}\omega^2, \\ L_1 &= (\omega_{10}^2 - \omega^2), \quad L_2 = (\omega_{20}^2 - \omega^2), \\ M_1 &= \delta_1 \omega, \quad M_2 = \delta_2 \omega, \end{aligned}$$

where δ_1 and δ_2 indicates the damping factors for bubbles 1 and 2, respectively. This equation is given by assuming the sphericity of bubbles and the incompressibility of the surrounding liquid same as in Eq. (1), while the damping factor is taken into account. When the damping factor is neglected, Eq. (2) is reduced to

$$\left(L_2 + \frac{R_{20}}{D}\omega^2\right) \left(L_1 L_2 - \frac{R_{10}R_{20}}{D^2}\omega^4\right) = 0,$$

and predicts that, regardless of the distance D , a bubble has three eigenfrequencies and, among those three frequencies, two correspond to those predicted by Eq. (1) (the terms in the second (\dots) correspond to those on the left hand side of Eq. (1)). Namely, two of the eigenfrequencies correspond to the natural frequencies, while that remaining has a different characteristic.

Figure 1 shows the eigenfrequencies, ω_1 and ω_2 , for $R_{10} = 5 \mu\text{m}$ and $R_{20} = 9 \mu\text{m}$ as functions of $D/(R_{10} + R_{20})$, given by Eq. (2). The partial natural frequencies are determined by

$$\omega_{j0} = \sqrt{\frac{1}{\rho R_{j0}^2} \left[3\kappa P_0 + (3\kappa - 1) \frac{2\sigma}{R_{j0}} \right]}, \quad \text{for } j = 1, 2,$$

where ρ ($= 1000 \text{ kg/m}^3$) is the density of the surrounding liquid, κ ($= 1.33$) is the specific heat ratio of the gas inside the bubble, P_0 ($= 1 \text{ atm}$) is the equilibrium pressure, σ ($= 0.0728 \text{ N/m}$) is the surface-tension coefficient.

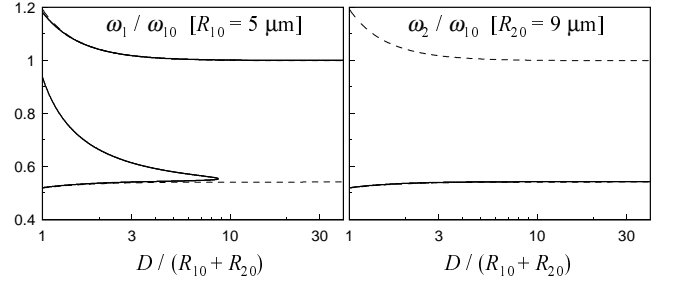


FIG. 1: Eigenfrequencies as functions of the distance between the bubbles (the solid lines). The dashed lines show the natural frequencies given by Eq. (1); it is hard to distinguish the higher one of bubble 1 and the lower one of bubble 2 from the eigenfrequencies since these frequencies overlap.

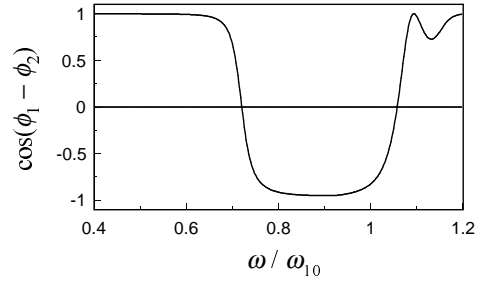


FIG. 2: Sign of the secondary Bjerknes force as a function of the driving frequency. The positive value indicates the attraction, while the negative value indicates the repulsion.

Since thermal conduction is not taken into account in the DNS technique [9], the damping factors are determined by the sum of the viscous and radiative ones as [3]

$$\delta_1 = \frac{4\mu}{\rho R_{10}^2} + \frac{\omega^2 R_{10}}{c} \quad \text{and} \quad \delta_2 = \frac{4\mu}{\rho R_{20}^2} + \frac{\omega^2 R_{20}}{c},$$

where μ ($= 1.137 \times 10^{-3} \text{ kg/(m s)}$) and c ($= 1500 \text{ m/s}$) are the viscosity and the sound speed, respectively, of the surrounding liquid. As discussed in Ref. [7], the highest and second highest eigenfrequencies of the larger bubble tend to vanish when the damping effect is sufficiently strong; in the present case, those disappear completely. The second highest and lowest eigenfrequencies of the smaller bubble cross and vanish at a certain distance, and only one eigenfrequency remains in the large-distance region.

The secondary Bjerknes force acting between two pulsating bubbles is represented by [1, 2, 3]

$$\mathbf{F} \propto K_1 K_2 E \frac{\mathbf{r}_2 - \mathbf{r}_1}{\|\mathbf{r}_2 - \mathbf{r}_1\|^3} \quad \text{with} \quad E \equiv \cos(\phi_1 - \phi_2),$$

where K_1 and K_2 are the pulsation amplitudes of the bubbles, \mathbf{r}_1 and \mathbf{r}_2 are their position vectors, and $\phi_1 - \phi_2$

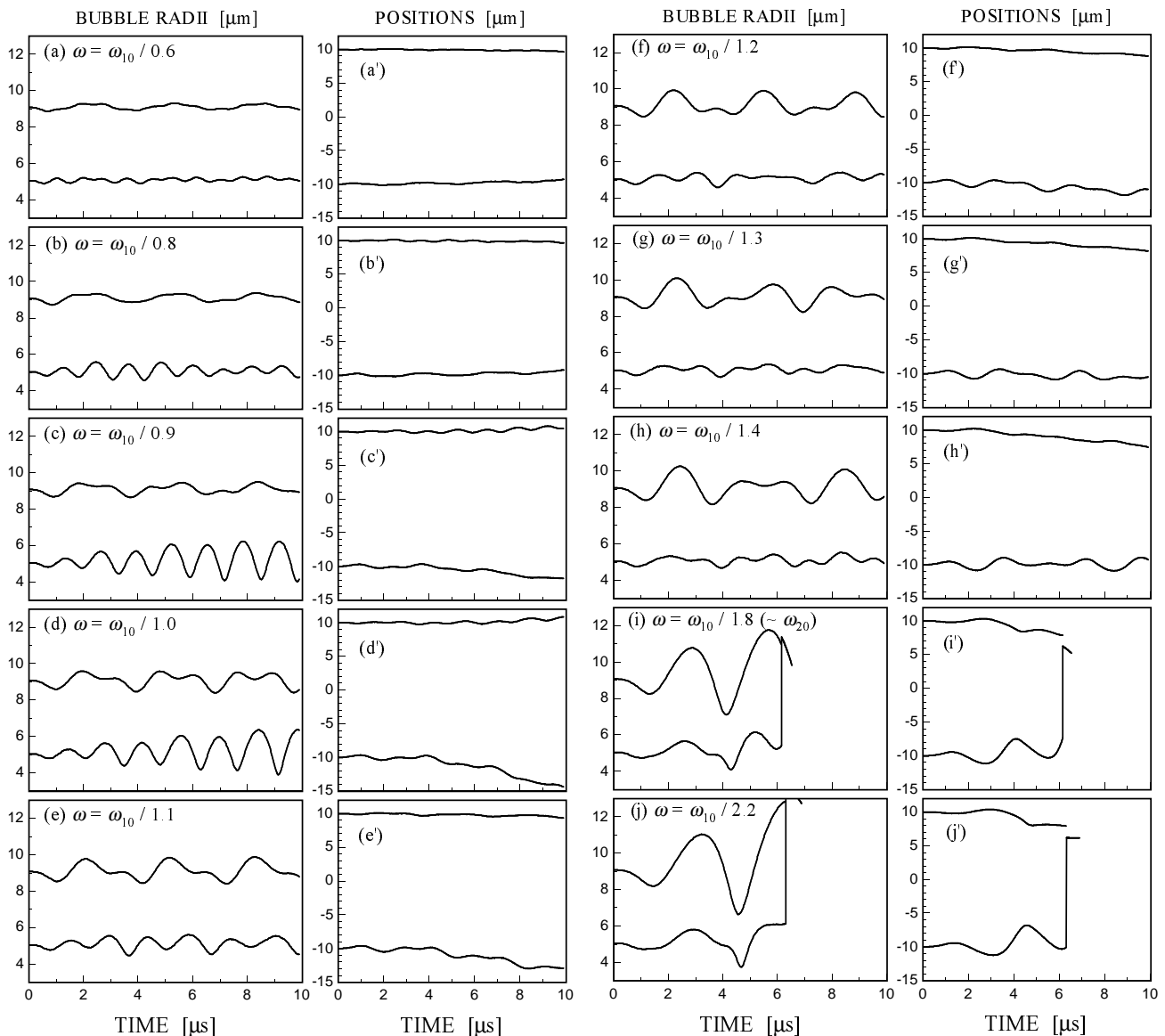


FIG. 3: Bubble radii [(a) ~ (j)] and corresponding positions [(a') ~ (j')] as functions of time for different driving frequencies, computed by the DNS technique. The lower lines in (a') ~ (j') denote the position of the smaller bubble. The coalescence of the bubbles takes place at the time where the number of the lines becomes one.

indicates the phase difference between them. (The concrete expressions for ϕ_1 and ϕ_2 are shown in Ref. [7].) The reversal of the sign of this force takes place only when the sign of E changes because $K_1 > 0$ and $K_2 > 0$ always [6, 7]. Figure 2 shows E as a function of the driving frequency. The physical parameters are the same as those used for Fig. 1, except for the distance fixed to $D = 20 \mu\text{m}$. In this figure, we can observe reversals at $\omega/\omega_{10} \approx 1.06$ and $\omega/\omega_{10} \approx 0.72$; respective reversals are

due to the highest and the second highest eigenfrequencies of the smaller bubble. The lowest eigenfrequency of the smaller bubble does not cause the reversal since the eigenfrequency of the larger bubble is almost equivalent to it and simultaneous phase reversal of both bubbles occurs; namely, a large phase difference between the bubbles does not appear in the frequency region around the lowest eigenfrequency.

III. NUMERICAL EXPERIMENTS

In this section, the DNS technique is employed to investigate the eigenfrequencies by observing the pulsation

amplitudes of the bubbles and the direction of the sec-

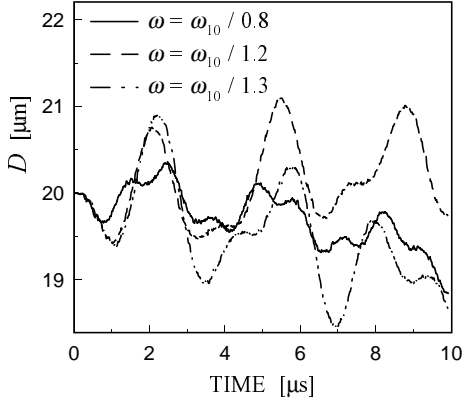


FIG. 4: Distance between the bubbles as functions of time for $\omega = \omega_{10}/0.8$, $\omega_{10}/1.2$, and $\omega_{10}/1.3$.

ondary Bjerknes force. The bubbles' radii and the initial distance between their mass centers are set by using the same values as those used for Fig. 2 [$R_{10} = 5 \mu\text{m}$, $R_{20} = 9 \mu\text{m}$, and $D(\text{time} = 0) = 20 \mu\text{m}$]. The content inside the bubbles is assumed to be an ideal gas with a specific heat ratio of 1.33, equilibrium density of 1.23 kg/m^3 , and viscosity of $1.78 \times 10^{-5} \text{ kg/(m s)}$. The surrounding liquid is water whose equation of state is determined by the Tait equation with an equilibrium density and pressure of 1000 kg/m^3 and 1 atm , respectively. The viscosity of water and the surface-tension coefficient are set to the same values as those used in Sec. II. The axisymmetric coordinate ($r \times z$) is selected for the computational space, and the mass centers of the bubbles are located on the central axis of the coordinate. The widths of the computational grids [Δr and Δz] are set as constant, being $\Delta r = \Delta z = 0.25 \mu\text{m}$, and the numbers of grids in the r and z coordinates are 100 and 320, respectively. The sound pressure, applied as the boundary condition to the pressure, is assumed to be in a form of $P_{ex} = P_a \sin \omega t$, where its amplitude P_a is set to be sufficiently low [fixed to 0.3 atm] and the driving frequency is selected from the frequency range around the bubbles' partial natural frequencies.

In Fig. 3, the bubbles' (mean) radii and positions as functions of time are displayed. From this figure, we know that the smaller bubble has two resonance frequencies, one of which is at $\omega \approx \omega_{10}/0.9$ and the other is at $\omega \approx \omega_{10}/2.2$. The former resonance frequency is higher than the partial natural frequency of the smaller bubble, and the latter is lower than that of the larger bubble ($\approx \omega_{10}/1.8$). These respective resonances may be due to the highest and the lowest eigenfrequencies of the smaller bubble, which correspond to the natural frequencies. The figure shows that the larger bubble has only one resonance frequency being at $\omega \approx \omega_{10}/2.2$. Those results are, at least in a qualitative sense, consistent with the theoretical result displayed in Fig. 1.

The sign of the interaction force changes twice in the

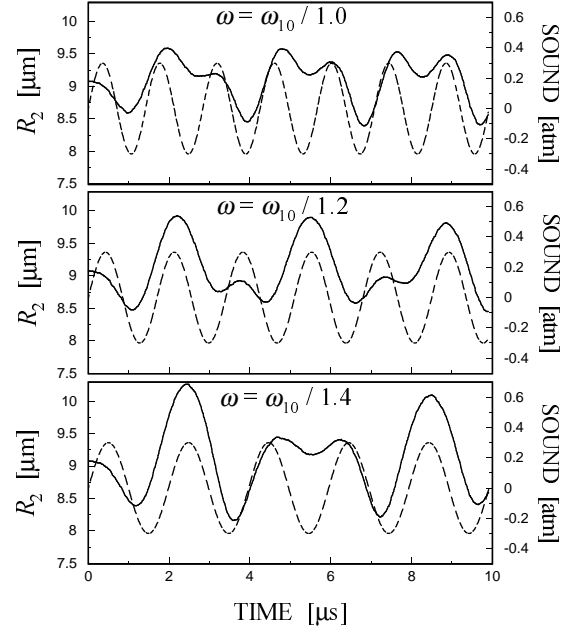


FIG. 5: Radius of the larger bubble (solid lines) and sound pressure as functions of time for different driving frequencies.

frequency region used. In the region between $\omega = \omega_{10}/0.8$ and $\omega = \omega_{10}/0.9$, being near the higher resonance frequency of the smaller bubble discussed above, the attractive force turns into repulsion as the driving frequency decreases, and, at $\omega \approx \omega_{10}/1.2$, the repulsive force turns into attraction. (Also see Fig. 4 which shows D in the cases where the deviation in D is small.) The former reversal is, obviously, due to the highest eigenfrequency of the smaller bubble. The question arises as to the cause of the latter one.

The latter reversal reveals that a kind of characteristic frequency should exist in the frequency region between the partial natural frequencies of the bubbles. It is evident that this characteristic frequency is not the resonance frequency of the larger bubble, which is much lower as discussed already. This result is in opposition to the assumption described by Doinikov and Zavtrak [5]. This characteristic frequency may be the second highest eigenfrequency of the smaller bubble as predicted by Ida [7]. (In Refs. [7, 8], it is proved that eigenfrequencies other than the natural frequencies do not cause the resonance response. This theoretical prediction is thoroughly reproduced in the present numerical results showing that the smaller bubble does not indicate a resonance response in this frequency region.) In order to confirm that this characteristic frequency is not that of larger bubble, we display in Fig. 5 the R_2 -time and P_{ex} -time curves for around $\omega = \omega_{10}/1.2$ in piles. This figure clearly shows that the pulsation phase of the larger bubble does not reverse in this frequency region; the bubble maintains its out-of-phase pulsation with the external sound

(the bubble's radius is large when the sound amplitude is positive), while other mode, which may come from the natural frequency of this bubble, appears.

IV. CONCLUDING REMARKS

In this paper, we have verified the recent theoretical results regarding the eigenfrequencies of two interacting

gas bubbles and the secondary Bjerknes force [6, 7]. The present numerical results given by the DNS technique support the theoretical results, at least in a qualitative sense. The use of models with higher accuracy [5, 15, 16, 17] rather than the classical coupled-oscillator model [4, 7, 14] used for the theory may allow us to acquire more quantitatively accurate results.

-
- [1] L. A. Crum, J. Acoust. Soc. Am. **57**, 1363 (1975).
 - [2] A. Prosperetti, Ultrasonics **22**, 115 (1984).
 - [3] W. Lauterborn, T. Kurz, R. Mettin, and C. D. Ohl, Adv. Chem. Phys. **110**, 295 (1999).
 - [4] E. A. Zabolotskaya, Sov. Phys. Acoust. **30**, 365 (1984).
 - [5] A. A. Doinikov and S. T. Zavtrak, Phys. Fluids **7**, 1923 (1995); J. Acoust. Soc. Am. **99**, 3849 (1996).
 - [6] M. Ida, (submitted); e-Print physics/0109005.
 - [7] M. Ida, (submitted); e-Print physics/0111133.
 - [8] M. Ida, (submitted); e-Print physics/0108056.
 - [9] M. Ida and Y. Yamakoshi, Jpn. J. Appl. Phys. **40**, 3846 (2001).
 - [10] M. Ida, Comput. Phys. Commun. **132**, 44 (2000).
 - [11] J. U. Brackbill, D. B. Kothe and C. Zemach, J. Comput. Phys. **100**, 335 (1992).
 - [12] M. Ida, (unpublished).
 - [13] S. Ito, 43rd Nat. Cong. of Theor. & Appl. Mech. (1994) p.311 [in Japanese].
 - [14] A. Shima, Trans. ASME, J. Basic Eng. **93**, 426 (1971).
 - [15] Yu. A. Kobelev and L. A. Ostrovskii, Sov. Phys. Acoust. **30**, 427 (1984).
 - [16] S. T. Zavtrak, Sov. Phys. Acoust. **33**, 145 (1987).
 - [17] A. A. Doinikov, J. Acoust. Soc. Am. **106**, 3305 (1999).